

## L-2-hydroxyglutaric aciduria: The role of neuroimaging in diagnosis

Published on 17.11.2022

**DOI:** 10.35100/eurorad/case.17933

**ISSN:** 1563-4086

**Section:** Neuroradiology

**Area of Interest:** Neuroradiology brain Paediatric

**Imaging Technique:** CT

**Imaging Technique:** MR

Case Type: Clinical Cases

**Authors:** Carolina Braga Chaves , Sílvia Reigada, Pedro Henrique Barradas

**Patient:** 3 years, male

### Clinical History:

A 3-year-old boy presented with a history of development delay, showing difficulties in the acquisition of words and sentence construction, and delayed capacity to walk without support. Parents concerns first began at 2 months of age because of hypotonia. Physical examination showed brachycephaly, ataxic gait and dysmetria.

### Imaging Findings:

Brain nonenhanced computed tomography (NECT) scan, requested because of craniosynostosis suspicion, revealed not only patent cranial sutures (figure 4a), but also abnormal hypodensities in the subcortical left parasagittal frontal white matter (WM) (figure 4b), in the posterior periventricular WM bilaterally (figure 4c), and in the dentate nuclei (figure 4d).

Subsequently, brain magnetic resonance imaging (MRI) showed multiple hyperintensities on fluid-attenuated inversion recovery (FLAIR) and T2-weighted images (T2WI), of the subcortical WM bilaterally, mainly in the frontal (figure 1a), parietal (figure 1b) and temporal lobes, with right-sided preponderance in the latter (figure 1c). Additionally, similar signal changes were found in the posterior periventricular WM (figure 1d), the globi pallidi (figure 2a), along the border of the putamina and caudate nuclei (figure 2a) and in the dentate nuclei (figure 2b). The observed lesions showed increased diffusivity on diffusion-weighted imaging (DWI) with elevation of the apparent diffusion coefficient (ADC) (Figure 3).

### Discussion:

#### Background

L-2-hydroxyglutaric aciduria (L-2-HGA) is a rare recessive autosomal inherited neurometabolic disease [1] caused by the accumulation of L-2-hydroxyglutaric acid (L-2-HG), a neurotoxic compound which causes leukoencephalopathy [1]. Increase of L-2-HG is the result of mitochondrial L-2-hydroxyglutarate dehydrogenase deficiency (L-2-HGDDH), which is due to mutations in the L2HGDH gene located on chromosome 14q22.12. The diagnosis is based on the substantially increased levels of L-2-HG in urine, blood or cerebrospinal fluid, complemented with brain MRI [3]. The genetic study confirms the diagnosis and establishes genotype guiding future genetic counselling [4].

## Clinical perspective

This disorder affects the central nervous system [1] and normally presents in the first years of life with developmental delay. Eventually, children experience a significant clinical deterioration, with progressive cerebellar ataxia and moderate to severe decline in cognitive function. Additionally, most patients have macrocephaly [6] and symptoms such as dystonia, tremor or seizures. L-2-HGA is also strongly associated with malignant brain neoplasms [3,5].

## Image perspective

MRI findings include subcortical leukoencephalopathy, affecting U-fibers [7], as well as changes in the dentate nuclei and basal ganglia, with high signal at T2WI/FLAIR and increased diffusivity in DWI. The combination of these findings, with sparing of deep WM and the corpus callosum, has been considered pathognomonic for L-2-HGA [8]. In our patient, the brain MRI gave rise to suspicion of the diagnosis of L-2-HGA by showing the typical involvement of subcortical WM combined with abnormal signs in the globus pallidus, putamen and dentate nucleus. The diagnosis was later confirmed by increase in L-2-HG urine levels (3497  $\mu$ mol/mmol creatinine; normal value: 0-40), and presence of c.907-2A>G mutation in L2HGDH gene in homozygosity. The pattern of WM involvement, and sparing of thalami and brain stem, are important towards restricting the differential diagnosis and help to distinguish L-2-HGA from Canavan disease or Kearns-Sayre syndrome [9], which normally have lesions of these structures. Canavan disease also has increased NAA in spectroscopy, which is pathognomonic for this disease [10].

## Outcome

There is no specific and effective treatment, but riboflavin and levocarnitine can stabilize the disease in some cases [11]. The prognosis is poor, although most patients reach adulthood.

## Take Home Message / Teaching Points

L-2-HGA is a rare inherited neurometabolic disorder.

It affects mostly children, causing neurodevelopmental delay and abnormalities in the neurological exam.

Neuroimaging findings include subcortical leukoencephalopathy, changes in dentate nucleus, globus pallidus and putamen.

Recognition of specific findings in the brain MRI, are instrumental in the differential diagnosis and should help guide biochemical and genetic study.

**Differential Diagnosis List:** L-2-hydroxyglutaric aciduria, Canavan disease, Kearns-Sayre syndrome

**Final Diagnosis:** L-2-hydroxyglutaric aciduria

## References:

- Vilarinho, L. et al. Novel L2HGDH Mutations in 21 Patients With L-2-hydroxyglutaric Aciduria of Portuguese Origin. *Hum. Mutat.* 26, 395–396 (2005).
- Rzem, R., Vincent, M.-F., Van Schaftingen, E. & Veiga-da-Cunha, M. L-2-Hydroxyglutaric aciduria, a defect of metabolite repair. *J. Inherit. Metab. Dis.* 30, 681–689 (2007).
- Haliloglu, G. et al. L-2-Hydroxyglutaric Aciduria and Brain Tumors in Children with Mutations in the L2HGDH Gene: Neuroimaging Findings. *Neuropediatrics* vol. 39 (2008).
- Steenweg, M.E., Jakobs, C., Errami, A., van Dooren, S.J., Adeva Bartolomé, M.T., Aerssens, P., Augoustides-

Savvapolou, P., Baric, I., Baumann, M., Bonafé, L., Chabrol, B., Clarke, J.T., Clayton, P., Coker, M., Cooper, S., Falik-Zaccai, T., Gorman, M., Hahn, A., Hasanoglu, A., King, M.D., de Klerk, H.B., Korman, S.H., Lee, C., Meldgaard Lund, A., Mejaški-Bošnjak, V., Pascual-Castroviejo, I., Raadhyaksha, A., Rootwelt, T., Roubertie, A., Ruiz-Falco, M.L., Scalais, E., Schimmel, U., Seijo-Martinez, M., Suri, M., Sykut-Cegielska, J., Trefz, F.K., Uziel, G., Valayannopoulos, V., Vianey-Saban, C., Vlaho, S., Vodopiutz, J., Wajner, M., Walter, J., Walter-Derbort, C., Yapici, Z., Zafeiriou, D.I., Spreeuwenberg, M.D., Celli, J., den Dunnen, J.T., van der Knaap, M.S. and Salomons, G.S. (2010), An overview of L-2-hydroxyglutarate dehydrogenase gene (L2HGDH) variants: a genotype–phenotype study. *Hum. Mutat.*, 31: 380-390

Patay, Z. et al. Cerebral Neoplasms in L-2 Hydroxyglutaric Aciduria: 3 New Cases and Meta-Analysis of Literature Data. *American Journal of Neuroradiology* vol. 33 (2012).

Divry, P. et al. L-2-Hydroxyglutaric Aciduria: Two Further Cases. *Journal of Inherited Metabolic Disease* vol. 16 (1993).

Shah, H., Chandarana, M., Sheth, J. & Shah, S. A Case Report of Chronic Progressive Pancerebellar Syndrome with Leukoencephalopathy: L-2 Hydroxyglutaric Aciduria. *Movement Disorders Clinical Practice* vol. 7 (2020).

Steenweg ME, Salomons GS, Yapici Z, Uziel G, Scalais E, Zafeiriou DI, Ruiz-Falco ML, Mejaski-Bosnjak V, Augoustides-Savvopoulou P, Wajner M, Walter J, Verhoeven-Duif NM, Struys EA, Jakobs C, van der Knaap MS. L-2-Hydroxyglutaric aciduria: pattern of MR imaging abnormalities in 56 patients. *Radiology*. 251(3):856-65 (2009).

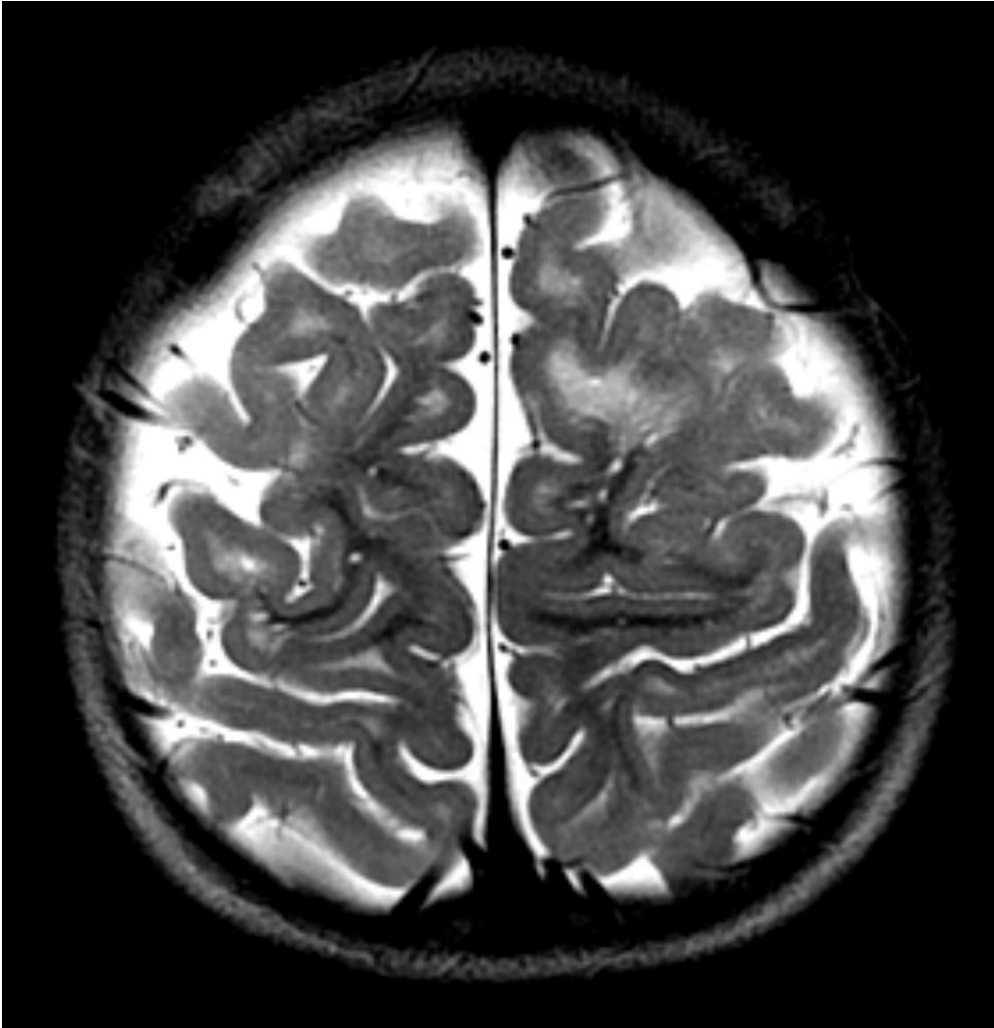
D'Incerti L, Farina L, Moroni I, Uziel G, Savoirdo M. L-2-Hydroxyglutaric aciduria: MRI in seven cases. *Neuroradiology*. 40(11):727-33 (1998).

Reddy N, Calloni SF, Vernon HJ, Boltshauser E, Huisman TAGM, Soares BP. Neuroimaging Findings of Organic Acidemias and Aminoacidopathies. *Radiographics*. 38(3):912-931 (2018).

Yilmaz, K. Riboflavin treatment in a case with L-2-hydroxyglutaric aciduria. *European Journal of Paediatric Neurology* vol. 13 (2009).

**Figure 1**

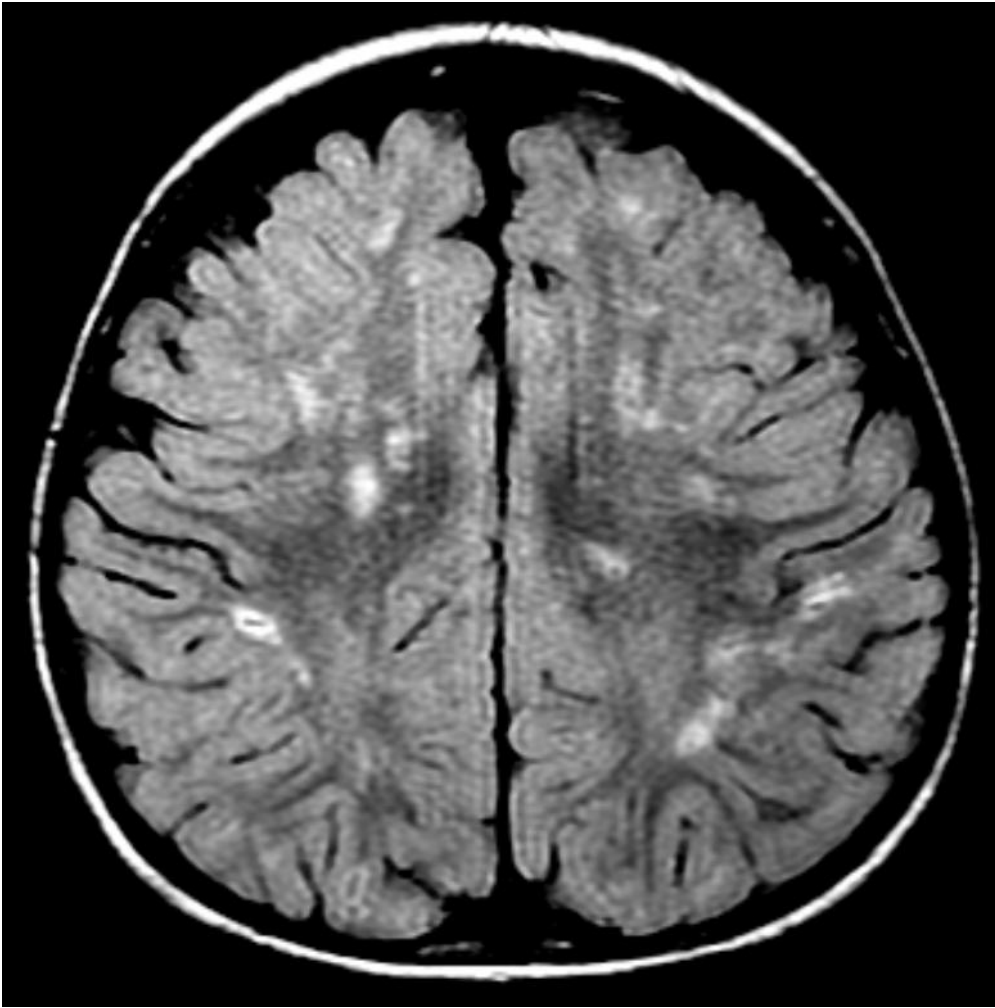
**a**



**Description:** Axial T2WI showed left superior frontal parasagittal subcortical WM hyperintensities

**Origin:** © Neuroradiology Functional Unit, Department of Imagiology, Centro Hospitalar e Universitário de Coimbra EPE, CHUC, Coimbra, Portugal, 2022

**b**



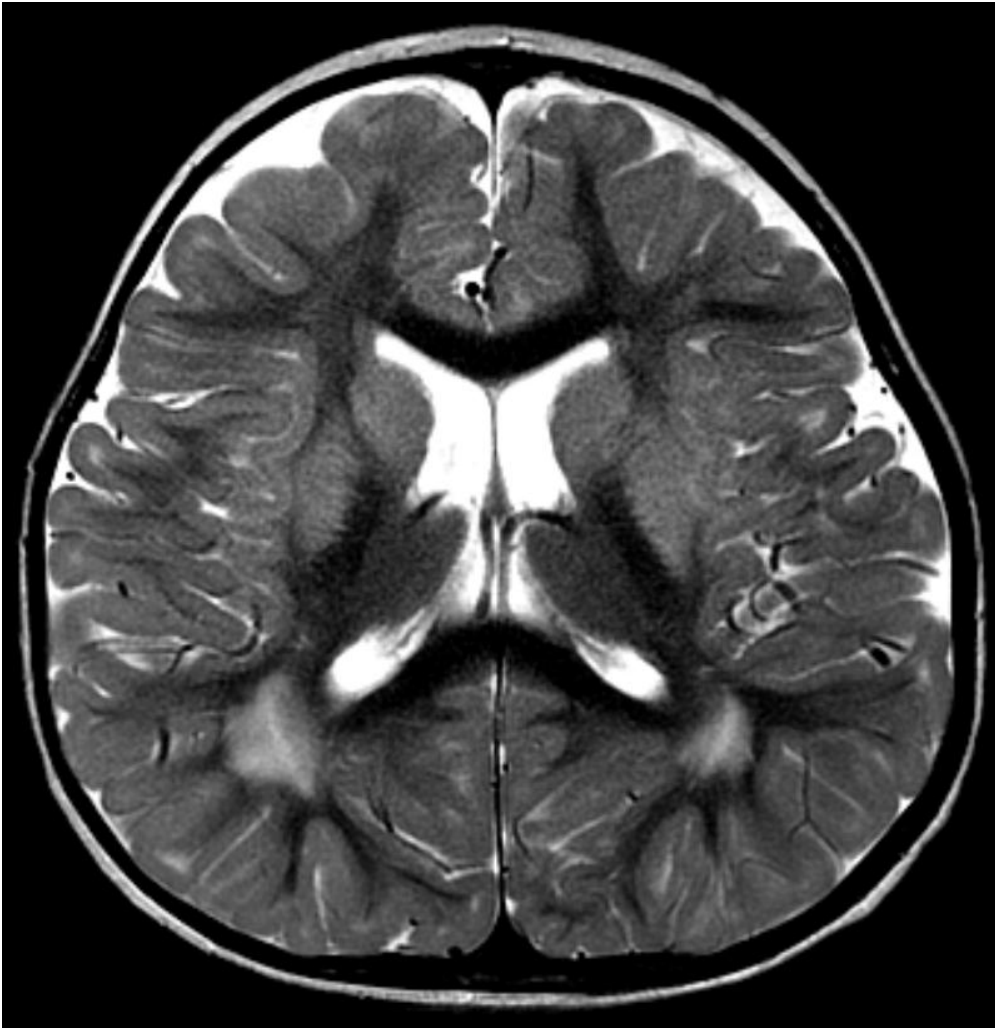
**Description:** Axial FLAIR presented bilateral hyperintensities of the frontoparietal and temporal subcortical WM, (c) more pronounced on the right in the latter. (d) Axial T2WI with hyperintensity of posterior periventricular WM bilaterally **Origin:** © Neuroradiology Functional Unit, Department of Imagiology, Centro Hospitalar e Universitário de Coimbra EPE, CHUC, Coimbra, Portugal, 2022

c



**Description:** Axial FLAIR presented bilateral hyperintensities of the frontoparietal and temporal subcortical WM, (c) more pronounced on the right in the latter. (d) Axial T2WI with hyperintensity of posterior periventricular WM bilaterally **Origin:** © Neuroradiology Functional Unit, Department of Imagiology, Centro Hospitalar e Universitário de Coimbra EPE, CHUC, Coimbra, Portugal, 2022

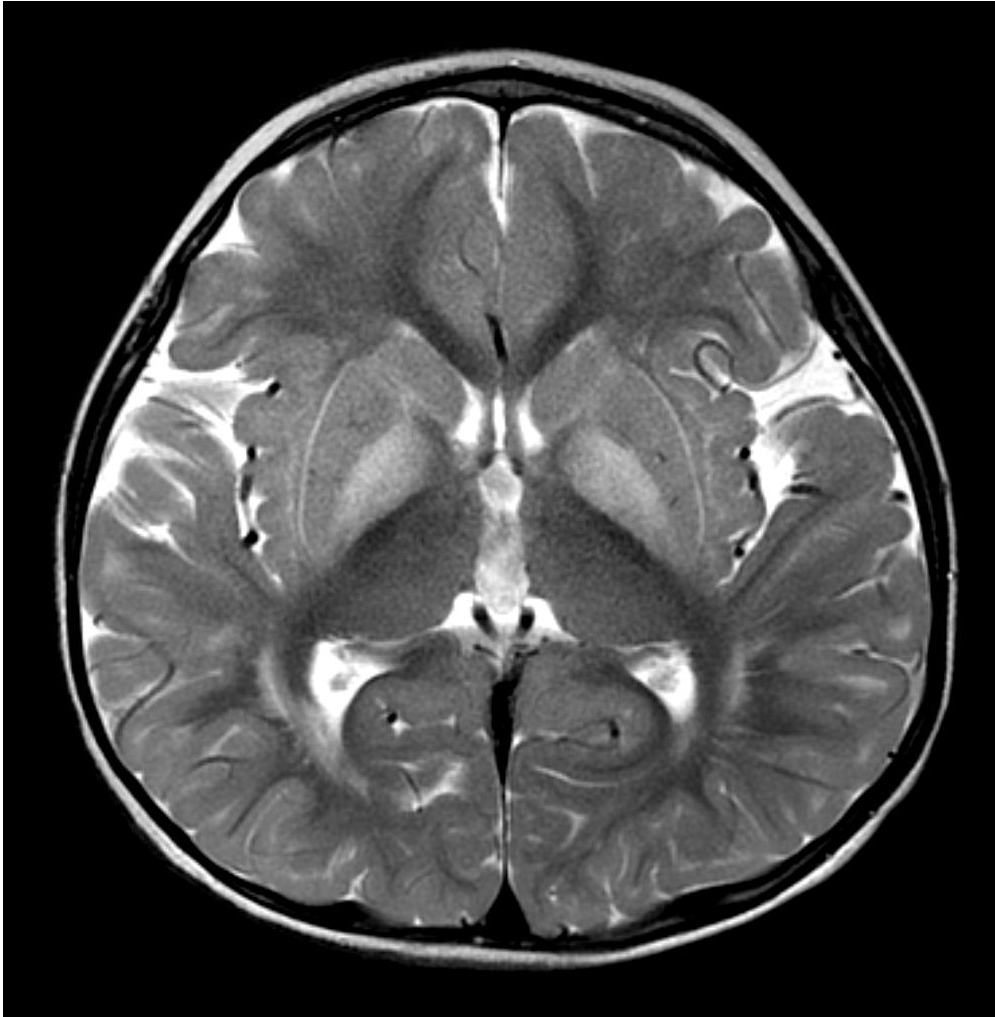
d



**Description:** Axial T2WI with hyperintensity of posterior periventricular WM bilaterally **Origin:**  
© Neuroradiology Functional Unit, Department of Radiology, Centro Hospitalar e Universitário de Coimbra EPE, CHUC, Coimbra, Portugal, 2022

**Figure 2**

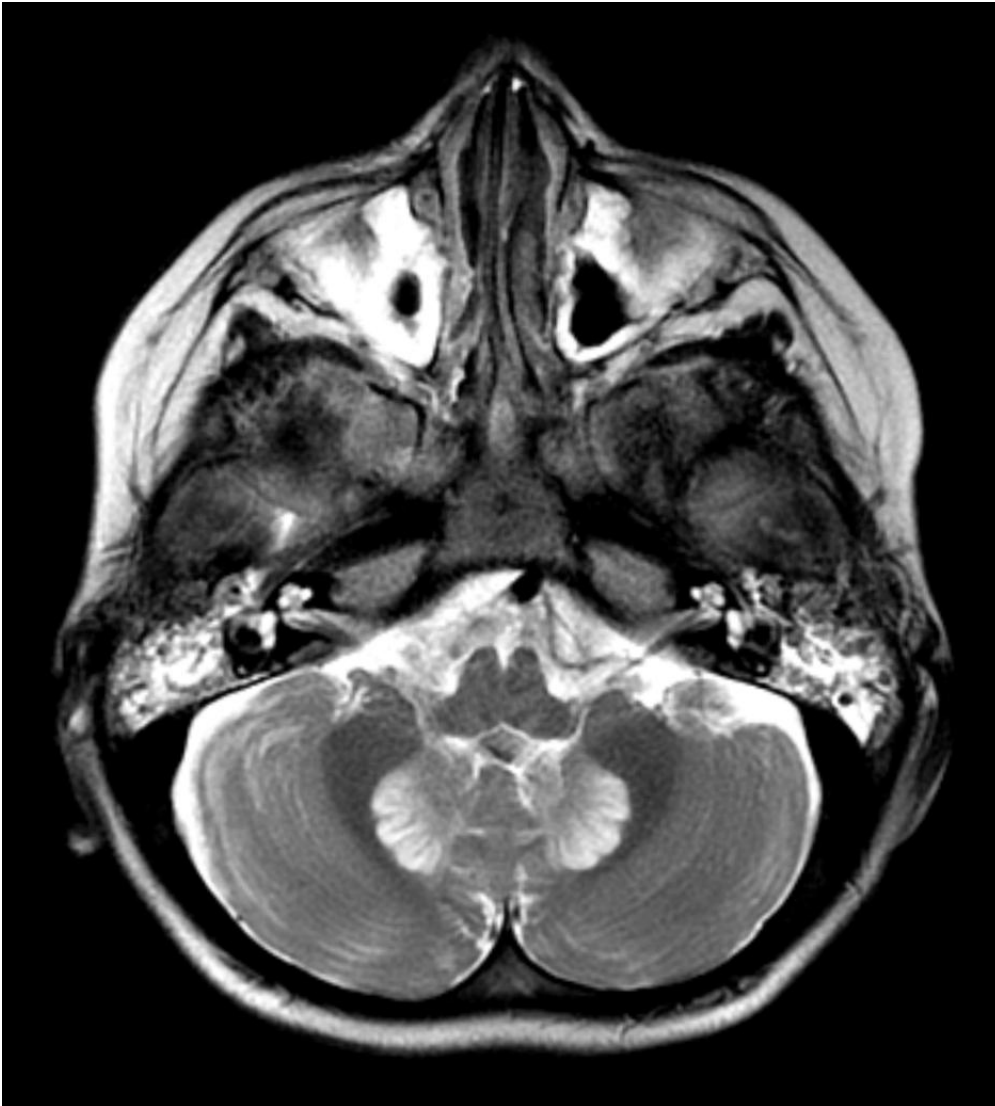
a



**Description:** Axial T2WI demonstrated hyperintensity of the globi pallidi, and a linear hyperintensity contouring the borders of both putamen and the head of the caudate nucleus **Origin:** © Neuroradiology Functional Unit, Department of Imagiology, Centro Hospitalar e Universitário de Coimbra EPE, CHUC, Coimbra, Portugal, 2022



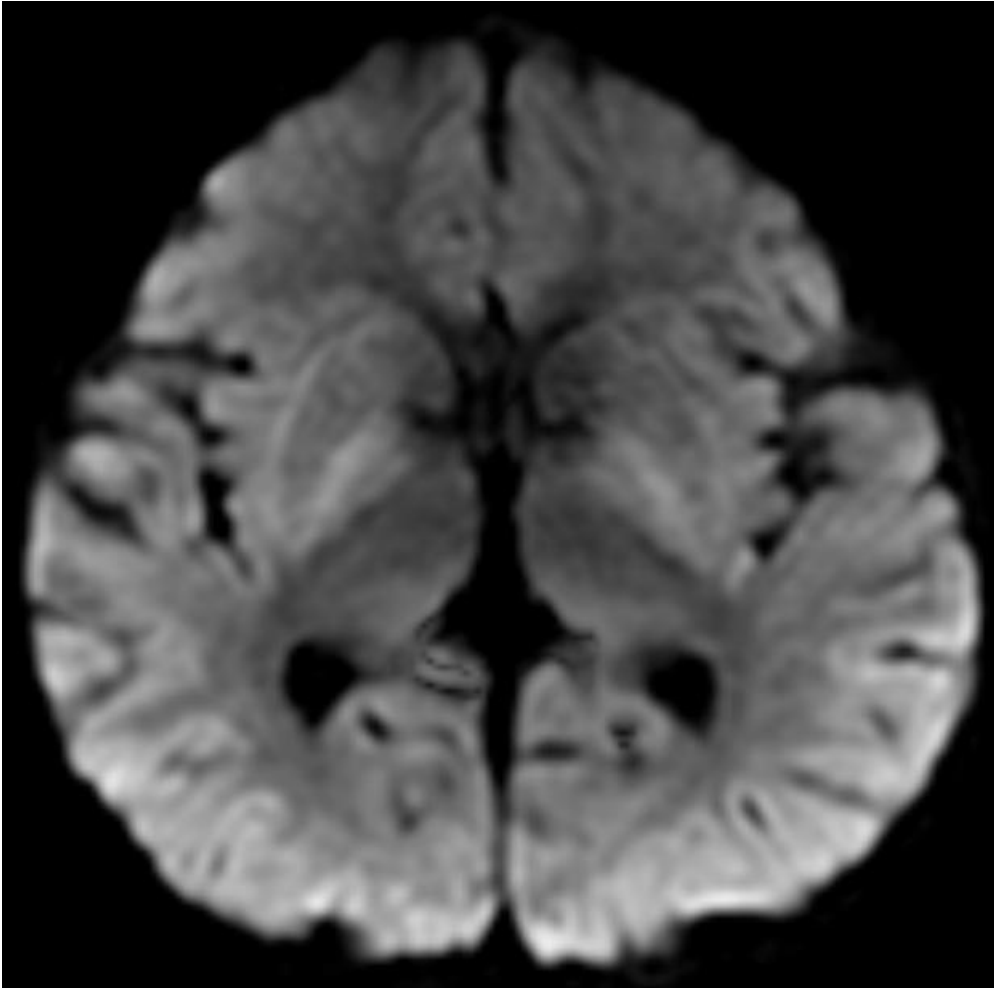
**b**



**Description:** Axial T2WI showed hyperintensity of dentate nucleus **Origin:** © Neuroradiology Functional Unit, Department of Imagiology, Centro Hospitalar e Universitário de Coimbra EPE, CHUC, Coimbra, Portugal, 2022

**Figure 3**

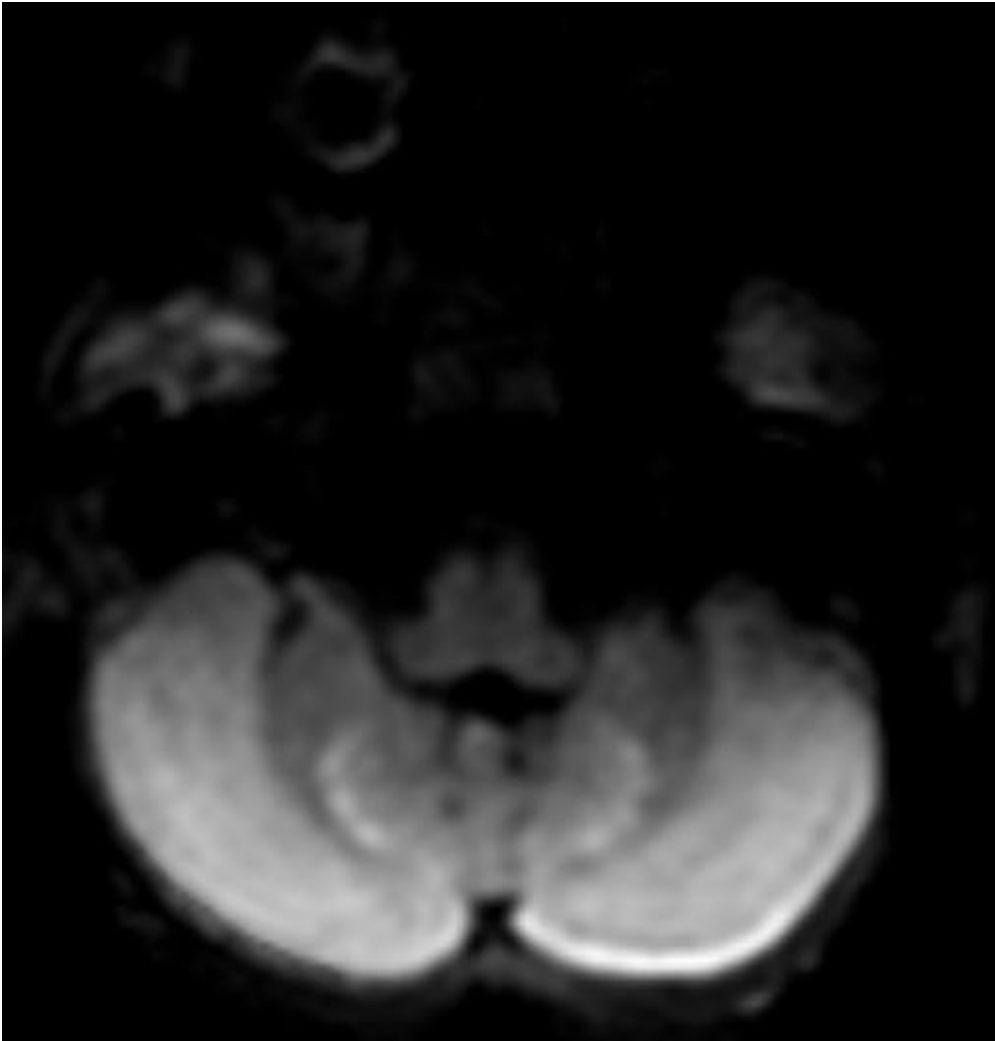
a



**Description:** Increased diffusivity on DWI of the globi pallidi and dentate nucleus with elevation of ADC

**Origin:** © Neuroradiology Functional Unit, Department of Imagiology, Centro Hospitalar e Universitário de Coimbra EPE, CHUC, Coimbra, Portugal, 2022

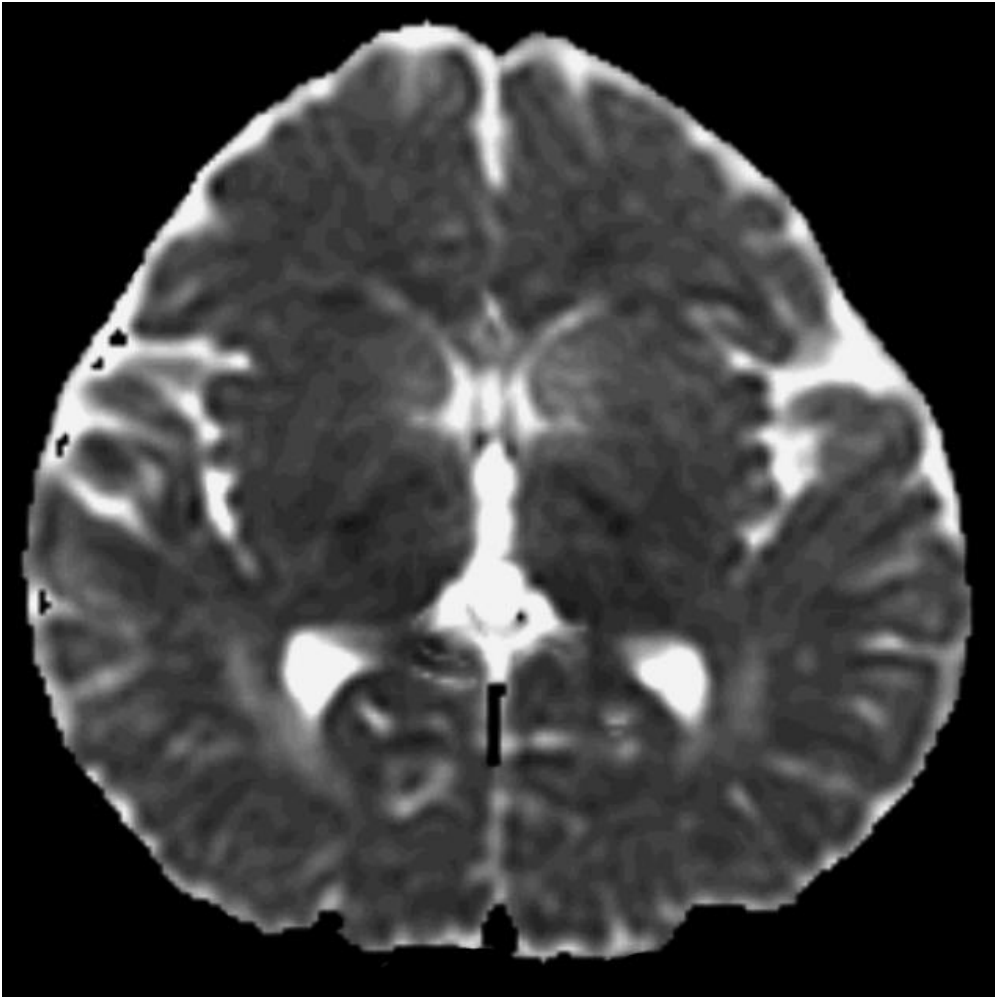
**b**



**Description:** Increased diffusivity on DWI of the globi pallidi and dentate nucleus with elevation of ADC

**Origin:** © Neuroradiology Functional Unit, Department of Imagiology, Centro Hospitalar e Universitário de Coimbra EPE, CHUC, Coimbra, Portugal, 2022

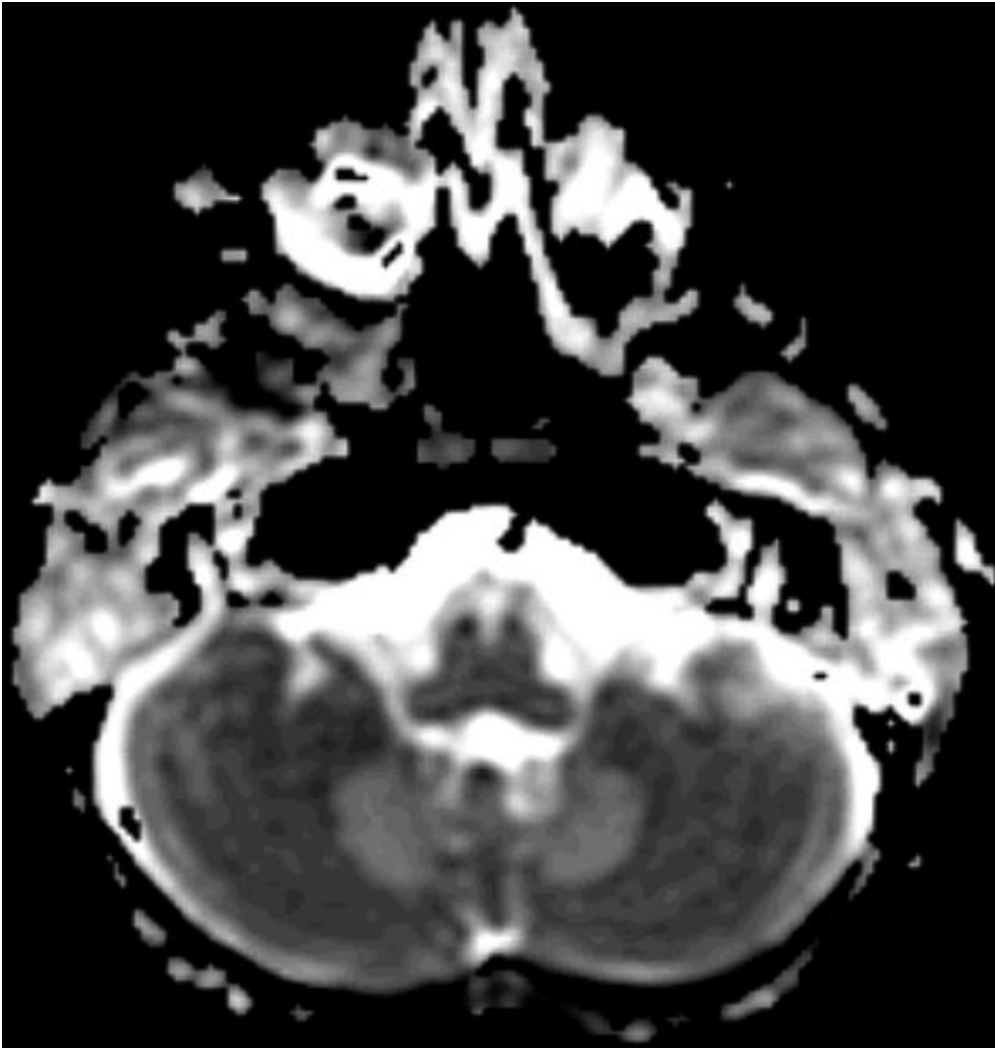
**c**



**Description:** Increased diffusivity on DWI of the globi pallidi and dentate nucleus with elevation of ADC

**Origin:** © Neuroradiology Functional Unit, Department of Imagiology, Centro Hospitalar e Universitário de Coimbra EPE, CHUC, Coimbra, Portugal, 2022

d



**Description:** Increased diffusivity on DWI of the globi pallidi and dentate nucleus with elevation of ADC

**Origin:** © Neuroradiology Functional Unit, Department of Imagiology, Centro Hospitalar e Universitário de Coimbra EPE, CHUC, Coimbra, Portugal, 2022

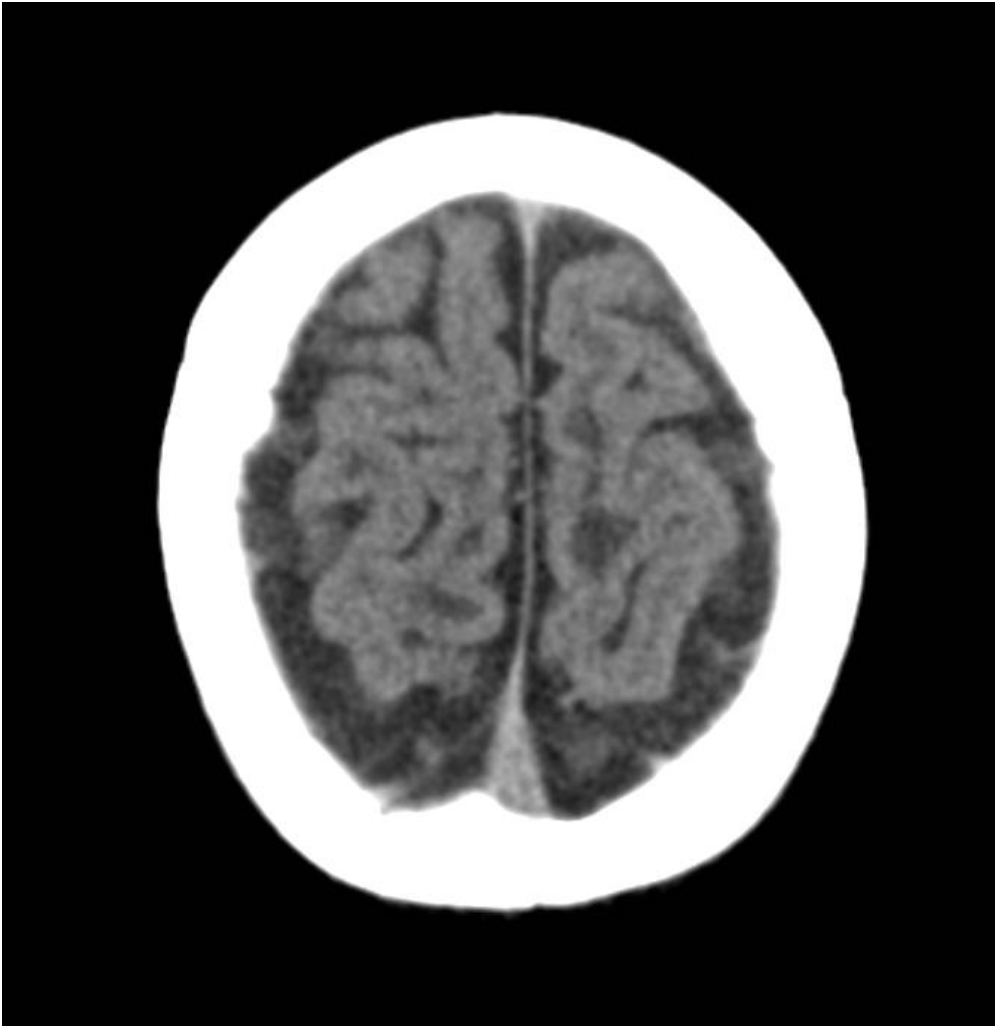
**Figure 4**

a



**Description:** Three-dimensional volume-rendered (VR) CT image showed sagittal and lambdoid patent cranial sutures **Origin:** © Neuroradiology Functional Unit, Department of Imagiology, Centro Hospitalar e Universitário de Coimbra EPE, CHUC, Coimbra, Portugal, 2022

**b**



**Description:** Left parasagittal frontal hypodense subcortical WM **Origin:** © Neuroradiology Functional Unit, Department of Imagiology, Centro Hospitalar e Universitário de Coimbra EPE, CHUC, Coimbra, Portugal, 2022

c



**Description:** Hypodensities of the posterior periventricular WM bilaterally **Origin:** © Neuroradiology Functional Unit, Department of Imagiology, Centro Hospitalar e Universitário de Coimbra EPE, CHUC, Coimbra, Portugal, 2022



d



**Description:** Symmetrical hypodensity of the dentate nucleus **Origin:** © Neuroradiology Functional Unit, Department of Imagiology, Centro Hospitalar e Universitário de Coimbra EPE, CHUC, Coimbra, Portugal, 2022